Symmetry-broken crystal structure of elemental boron at low temperature

M. Widom

Department of Physics, Carnegie Mellon University, Pittsburgh, PA, USA

M. Mihalkovič

Institute of Physics, Slovak Academy of Sciences, Bratislava, Slovakia

(Dated: November 6, 2007)

The crystal structure of boron is unique among chemical elements, highly complex, and imperfectly known. Experimentalists report the β-rhombohedral (black) form is stable over all temperatures from absolute zero to melting. However, early calculations found its energy to be greater than the energy of the α-rhombohedral (red) form, implying β cannot be stable at low temperatures. Furthermore, β exhibits partially occupied sites, seemingly in conflict with the thermodynamic requirement that entropy vanish at low temperature. Using electronic density functional theory methods and an extensive search of the configuration space we find a unique, energy minimizing pattern of occupied and vacant sites that can be stable at low temperatures but that breaks the β-rhombohedral symmetry. Even lower energies occur within larger unit cells. Alternative configurations lie nearby in energy, allowing the entropy of partial occupancy to stabilize the β-rhombohedral structure through a phase transition at moderate temperature.

PACS numbers: 61.66.Bi

I. INTRODUCTION

Elemental boron is important for its light weight, high strength, high melting point and semiconducting properties. It is also intrinsically interesting owing to its complex structures which are characterized by their arrangements of icosahedral clusters. Boron is almost unique among elements in lacking a well understood and universally agreed upon low temperature structure. Knowledge of the precise structure is required for understanding its remarkable electronic and mechanical properties, and also for understanding the stability of technologically important boron compounds relative to their constituent elements.

The first reported crystallographic refinements of elemental boron were the α-tetragonal [1, 2] and α-rhombohedral forms [3, 4]. Although the α-rhombohedral form was initially believed stable at low temperature [3], the β-rhombohedral form, was later discovered [5] and proposed as the true low temperature state. Still later, the β-tetragonal form was discovered and its crystal structure refined [6]. The α and β-rhombohedral structures are illustrated in Figs. 1 and 2 and are described in greater detail in Section I A.

The debate over the proper stable form of boron continues today, with some researchers suggesting α-rhombohedral is the true low temperature state [7]. In particular, the calculated energy of α lies below the reported calculated energies of β [7–10]. Some researchers propose a finite temperature phase transition [11], including one proposal that vibrational entropy drives an α to β transition at finite temperature [7]. Quantum mechanical zero point vibrational energy has been proposed as a mechanism to stabilize the β-rhombohedral form at absolute zero [10].

We note that the β-rhombohedral form exhibits intrinsic disorder in the form of partially occupied sites. Partial occupancy occurs in crystallographic refinement when the site is occupied, at a given instant, in some copies of the unit cell but not in others. Within a single unit cell the site may be occupied at some times but not at others. Since thermodynamics requires that entropy vanish in the limit of low temperature, and partial occupancy implies finite entropy, the partially occupied β-rhombohedral form is not a plausible low temperature structure. Correlations among the partially occupied sites of β must favor a unique pattern of occupancy that minimizes the energy.

We carry out an extensive study of the configuration space that explores specific resolutions of partial occupancy, assigning atoms or vacancies to specific sites. Our results indicate that a particular symmetry-broken form of β achieves energy lower than α and thus is the true low temperature structure. A symmetry restoring phase transition, driven by the high entropy of an ensemble of nearly degenerate configurations, should occur at a moderate temperature, explaining the experimental observation of β-rhombohedral as the equilibrium phase at higher temperatures.

The remainder of this introduction briefly describes the known structures of crystalline boron and our calculational methods. Results are presented in Section II. We find optimal assignemnts of atoms to partially occupied sites, we validate these findings using solid state molecular dynamics simluations, and we explore possible superlatttice ordering. Finally we discuss our conclusions in Section III.

A. Structural description

Crystalline boron occurs primarily in tetragonal and rhombohedral forms. Since the tetragonal forms are known to be metastable, our analysis in this paper focuses on the rhombohedral forms. Both the α and β-rhombohedral forms share a common space group, $R\bar{3}m$ (group # 166). Three rhombohedral primitive cells combine to form a larger nonprimitive hexagonal unit cell with three times the number of atomic sites. The rhombohedral (111) axis becomes the hexagonal symmetry axis of the hexagonal unit cell. For simplicity our analysis is based on the rhombohedral primitive cell, though we do at the end consider supercells of the primtive cell including the full hexagonal unit cell.

Structure types are denoted by their Pearson symbols. For example, Pearson type tP50 (α-tetragonal) is primitive tetragonal with 50 atomic sites per cell. Pearson tP196 (β-tetragonal) is also primitive tetragonal but with 196 atomic sites per unit cell. Because of partial occupancy tP196 actually has fewer than 196 atoms distributed among its 196 sites. Pearson hR12 (α-rhombohedral) and hR105 (β-rhombohedral) are both rhombohedral primitive cells of 12 and 105 sites repsectively. Three rhombohedral primitive cells may be combined to form a single hexagonal cell.

All crystalline boron structures share a common structural motif, the 12-atom icosahedral cluster. Various allotropes differ in the spatial arrangement of the icosahedra and in the presence of interstitial atoms. The structural complexity of boron is due to the "electron deficiency" of the B_{12} icosahedral cluster [12, 13] which frustrates the distribution of electrons among available bonds. Presumably the partial site occupancy serves to relieve this frustration [14].

Among boron allotropes, α-rhombohedral boron has the simplest structure (see Fig. 1), with a B_{12} icosahedral cluster placed at each vertex of the rhombohedral cell. The structure is defined by just two independent Wyckoff positions [15]. The icosahedral clusters are nearly regular, with bond lengths in the range of 1.75-1.81 Å. Clusters are joined along six of their twelve 5-fold axes that point radially outwards through vertices of the icosahedron.

These intericosahedral bonds have length 1.67 Å. Also visible in the figure are bonds of length 2.01 Å running parallel to the icosahedral 2-fold axes. This bond length is almost completely absent in all other allotropes, so we believe it is energetically unfavorable.

The β-rhombohedral structure (see Fig. 2) differs from α in that the icosahedral cluster at the origin joins to twelve other icosahedra along each of its twelve five-fold axes. In contrast to α, where all icosahedra share a common orientation, in β the twelve surrounding icosahedra are each rotated by 36° relative to the central icosahedron around their common axes. Consequently, the lattice constant of β is approximately double that of α. As shown, the icosahedra shaded in blue are at positions equivalent to those in the α structure, while those shaded in red are new.

Another new feature in β is the presence of partially occupied sites. Although the original hR105 structure model [5, 16] contained 15 Wyckoff positions, each fully occupied, an intermediate model [17, 18] (Pearson type hR111) assigned the B13 position 73% average occupancy and introduced a new B16 position at 25% occupancy (the numbering scheme we use is common to all the cited authors). In the Pearson type hR141 model [19] illustrated in Fig. 2, the B13 position is listed at 74.5% average occupancy, the B16 position at 27.2%, and additional positions B17, 18, 19 and 20 are given occupancies of 8.5%, 6.6%, 6.8% and 3.7% respectively. Other than the B20 position, all partially occupied positions lie in mirror planes of the structure that contain the rhombohedral (111) axis. They appear as collinear sets in the projections shown in Figs. 2 and 3.

B. Methods

Our basic calculational methods follow Ref. [8]. The calculations use the electronic density functional program VASP [20] version 4.6.28. VASP uses a plane-wave approach that relies on periodic boundary conditions and is well suited to the study of periodic crystal structures. Electron-ion interactions are represented using Projector Augmented Wave (PAW) potentials [21, 22] which are an all-electron generalization of pseudopotentials. For boron the 1s electrons are treated within the ionic core while the 2s and 2p electrons are assigned to the valence band. All structures considered were electrically neutral.

The exchange-correlation functional is taken as the PW91 Generalized Gradient Approximation (GGA) [23]. Previously the GGA has been shown superior to LDA (the Local

Density Approximation) for studies of Boron clusters and compounds [24, 25], with accuracy nearly that of Hartree-Fock calculations at the self-consistent-field (SCF) level [26].

All structures are fully relaxed, both in atomic coordinates and lattice parameters, subject to the preservation of initial symmetry, using a conjugate gradient algorithm. Owing to coupling of the basis set to the volume we perform consecutive calculations (i.e. stop and restart) to fully relax the structure. Reported energies are obtained from a final static calculation.

We test the dependence of energy *differences* among the α, β-rhombohedral and optimized symmetry-broken β (see section II B) structures on computational parameters. The results are summarized in table II. To maintain consistent cell sizes we use a 2x2x2 supercell of the α phase, whose lattice parameters become similar to those of β. The plane wave energy cutoff E_{cut} is 319 eV by default, and we also test 415 eV. "Precision" settings of "Medium" and "Accurate" set the density of FFT grids which control wrap-around errors. We systematically increase the Monkhorst-Pack k-point mesh starting from 1x1x1 (i.e. the Γ-point) until sufficient convergence is achieved. Based on the data presented we claim energy differences are converged to within 6% (roughly two significant figures) provided we use a k-point mesh of 3x3x3 and "Accurate" precision. The default plane wave energy cutoff of 319 eV suffices.

In Table III we test the dependence on choice of potential and exchange-correlation functional. The local density approximation [27] (LDA) is expected to be the least accurate method. The ultrasoft pseudopotential method [28] (USPP) treats only the valence electrons explicitly. The "hard" potential has a very small core radius and correspondingly high E_{cut}=700eV. Results with this potential are expected to be comparable in accuracy to all-electron FLAPW calculations and to Gaussian with large basis sets, according to VASP documentation [29].

Because our final energy difference $E_{opt} - E_{\alpha}$ is not much larger than the variation among the GGA calculations it would be desirable to repeat this calculation using more refined quantum-chemical methods. However, all methods agree that our optimized structure achieves a lower energy than α, with the exception of LDA which is expected to be the least accurate. Even if a more accurate calculation were to find that *all* variants of β were higher in energy than α, that would not alter our central conclusion that the fully symmetric β-rhombohedral structure is a high temperature phase stabilized by occupancy fluctuations.

II. RESULTS

Total energy calculations depend on precise knowledge of atomic positions, with partially occupied sites resolved into a specific pattern of occupied or vacant positions. Likewise partial site occupancy is thermodynamically forbidden in the $T = 0K$ limit. Hence we explore the ensemble of likely instantaneous configurations, seeking both the unique optimal arrangement of atoms among partially occupied sites as well as an estimate of the entropy associated with nearly optimal configurations. We carry out the study initially within a single rhombohedral primitive cell, repeated infinitely owing to the periodic boundary conditiions. Later we study superlattice ordering within supercells.

Table I lists our main results [30]. Energies are given relative to the α-rhombohedral form, which we take as a reference because it contains no partial occupancy and was previously the lowest energy structure that was known. As expected, the tetragonal structures, known to be metastable, exhibit relatively high energies. The fully occupied hR105 β-rhombohedral structure is higher in energy than the α-rhombohedral hR12 structure, as previously noted [7–10]. If β is to be stable at low temperatures it must involve the placement of atoms among the partially occupied sites of hR111 or hR141. Some particular pattern of occupied and vacant sites must minimize the total energy while breaking the rhombohedral symmetry.

The following tables present energy data supporting specific conclusions on the optimization of B.hR111 and B.hR141. Figures and atomic coordinates for each named structure, and many other structures not listed here, can be viewed at our web site [30] (see the special "published" area). Data is shown for symmetry-inequivalent structures. All energies are given for a 3x3x3 Monkhorst-Pack k-point mesh, for accurate precision and the standard PAW potential with default plane wave energy cutoff of 319 eV as discussed in Section I B.

The notation lists only those sites among the partially occupied Wyckoff positions that are actually occupied. Positions B1-B12, B14 and B15 are always fully occupied and thus are not listed in our notation. The hR111 structure introduces partial occupancy at B13 and the new B16 position. The hR141 structure introduces additional positions B17-B20. The notation $abcdef$ refers to specific sites within each Wyckoff position, as labeled in Fig 3.

A. Pearson hR111

We first explore the hR111 model [18]. The two partially occupied sites, B13 and B16 are both of Wyckoff type 18h, meaning that 18/3=6 of these sites occur per rhombohedral primitive cell. The B13 sites form a pair of equilateral triangles surrounding the B15 site at the primitive cell body center (see light blue atoms in Fig. 3). The B16 sites form a pair of equilateral triangles that lie immediately above faces of the icosahedra at primitive cell vertices (see pink atoms in Fig. 2).

A B13 atom can be swapped for a B16 atom in 4 symmetry-inequivalent ways, each of which lowers the energy by 12-13 meV/atom. This substitution is thus strongly preferred energetically, but the spatial correlation between occupied and vacated site is relatively weak, as suggested by Slack [19].

Since the number of atoms per cell is believed to be greater than 105, we also considered a single B13 vacancy and a pair of B16 atoms, again exhaustively testing all combinations. Low energy requires that one atom reside on each equilateral triangle of B16. Our optimal structure within the confines of hR111 is B13bcdefB16bd, at an energy of 0.15 meV/atom above hR12. The B13bcdefB16bf structure was the best found in a previous study by van Setten, et al [10].

B. Pearson hR141

So far the occupancy of B13 is larger than reported experimentally, the energy remains above the energy of α, and the total number of atoms per primitive cell remains below the experimentally reported value of 106.7. Evidently we should try removing another atom from B13 and placing that atom (and more) at other locations. To place these atoms we utilize the additional partially occupied positions of hR141, namely B17-20. There are of order 10^6 distinct arrangements of atoms within a single primitive cell that are consistent with experimentally observed occupancies. Since this is far too many structures to explore exhaustively, we build upon our prior results and consider other likely correlations in order to focus our search.

Following Slack [19] we note the 1.57 Å bond between B13 and B17 sites is slightly too short for simultaneous occupancy. If we choose to occupy B17a, this model suggests that B13d and B13e should be vacant. However, our calculations show this arrangement is not stable. One of the vacancies moves to the B13a site leaving just a single vacancy on either B13d or e but not both. Then the B17a atom relaxes to accommodate the bond to the remaining nearby B13 atom, which ends up at length 1.86 Å. It is noteworthy that the B17 site reports an anomalously large thermal Debye-Waller factor, indicating large displacements from the refined position. We suggest that this position should be split into distinct sites whose occupancy is correlated with the nearby B13. In fact, Slack utilized an alternative split site "B17d" to refine one of his samples, and one of these B17d sites lies within 0.1 Å of our relaxed B17 position.

The 1.62 Å bond length between sites B17 and B18 is within the favorable range, and their reported occupancies are similar, so we presume their occupation is correlated. Our calculated energies confirm this, with a reduction in energy of 1.1 meV/atom upon introduction of an atom at the B18 site adjacent to an occupied B17 site. After optimizing the placement of B16 atoms this leads to our optimal primitive cell structure, B13bcefB16bdB17aB18a, which contains 107 atoms and achieves an energy 0.86 meV/atom below the energy of α. This model also achieves a close match of relaxed positions to experimentally observed positions, as is evident from the ΔR values in Table I.

The B19 and B20 sites so far remain unused in our study. B19 sites are only 0.74 Å away from B18 sites, so these may never be simultaneously occupied. Both B19 and B20 sites lie close to the centers of fully occupied hexagonal rings, resulting in small patches of triangular lattice that are atypical of crystalline boron structures (although they may be stable in small boron clusters and nanotubes [31]). We found no significantly low energy structures utilizing B19 or B20 sites. Van Setten et al. [10] report a low energy for B19bcdefB16eB19a, but we find this is not favorable. Rather the B19a atom relaxes to the nearby B17a position.

C. Molecular dynamics

Because we cannot systematically evaluate all configurations within the hR141 primitive cell, we checked our result using molecular dynamics. We used the VASP-calculated forces to perform molecular dynamics simulations of a single primitive of β. To achieve atomic diffusion we employed a high temperature T=2000K (melting is around T=2365K). We estimated the lattice parameters as a=11.047 Å and c=24.155 Å based on an experimental report of thermal expansion [32].

We ran samples of 106, 107 and 108 atoms for a duration of 16ps each, using 1fs time steps. To search for optimal configurations we drew instantaneous configurations from the molecular dynamics run every 2ps and quenched them. To carry out the quench we rescaled the lattice parameters to their crystallographic values and performed molecular dynamics with a linearly decreasing temperature ramp that reached T=300K after 3ps. We then performed conjugate gradient relaxation to reach 0K. This procedure was able, on occasion, to achieve the optimal structures we reported, but usually resulted in higher energies.

Fig. 5 shows a density plot of atomic positions for the 107 atom run that started with our optimal structure as an initial condition. Densities have been averaged to impose rhombohedral symmetry. Sharing of atoms between B13 and B17 positions is clearly visible, as is partial occupation of B18 and B16 positions.

D. Supercell studies

Although we optimized the assignment of partial occupancy within a single hR141 primitive cell, there is a possibility of a lower energy structure within either the hexagonal unit cell (Pearson type hP423) or some other supercell of the primitive cell.

The hexagonal unit cell (Pearson type hP423, dimensions a=10.9 Å, c=23.8 Å) contains three copies of the rhombohedral primitive cell stacked in the direction parallel to the rhombohedral (111) axis. We consider the case where each primitive cell is identically decorated, where one is rotated by 120° relative to the other two, and where each is rotated by 120° relative to its neighbors. In this last case a 3_1 screw axis is introduced. In Table VI energies are given for a 3x3x1 k-point mesh with medium, maintaining a uniform reciprocal space density comparable to a 3x3x3 mesh for a single primitive cell. It appears energetically preferable to maintain identical orientations of all vertically stacked cells.

However, within a 2x1x1 supercell of the 107 atom primitive cell, which places independent primitive cells adjacent to each other (see Fig. 4), we did find superstructures which lowered the energy significantly. To describe these we focus on a motif near the center of our optimal primitive cell structure. One of the two B13 vacancies is collinear with the occupied B17 and B18 sites (e.g. B13aB17aB18a). The second B13 vacancy is adjacent to the first (e.g. B13d). This motif of collinear and adjacent sites can occur in six rotated variants and six more that are reflected versions.

We examined all 22 symmetry-inequivalent arrangements of this motif within the 214 atom supercell. For each arrangement we optimized the placement of the B16 atoms. The relative arrangements are coupled mainly by the placement of B16 atoms, and all energies lay within 2 meV/atom of each other. Energies are given in Table VII for a 1x3x3 k-point mesh and precision set to "Accurate". Several supercell structures yielded energies lower than the optimal 107 atom structure, indicating a preference for superlattice ordering at low temperatures, with adjacent cells of β resolving their partial occupancy with differing orientations of a common motif.

The large number of nearly degenerate configurations suggests the possibility of a phase transition from the symmetry-broken low energy structure to a state that restores the β-rhombohedral symmetry by sampling the full ensemble of motif orientations. To judge the chance of such a phase transition, we evaluate the partition function of our 2x1x1 supercell

$$Z = \sum_{\alpha} \Omega_{\alpha} e^{-E_{\alpha}/k_B T} \tag{1}$$

where α runs over all 22 symmetry-independent configurations, Ω_{α} is the multiplicity of the configuration and E_{α} is the relaxed energy, optimized over placements of B16 atoms (as in Table VII but multiplied by 214 for the number of atoms per supercell).

Thermodynamic derivatives of Z yield the internal energy U, the entropy S and the heat capacity C. The heat capacity exhibits a strong peak around $T = 300K$. Fig 6 plots thermodynamic data resulting from this model. The strong peak around T=300K represents the unlocking of the relative orientations of our collinear motif (see above). The small heat capacity peak around T=50K represents the unlocking of the second B13 vacancies (see above) while holding the collinear motif fixed. The entropy available from unlocking dominates the energy cost, substantially lowering the free energy. Based on this it seems likely that in an infinite system there should be a symmetry-restoring phase transition at a moderate temperature, driven by the entropy of suboptimal occupation patterns of the partially occupied sites. This transition may be difficult to observe experimentally because atomic diffusion is slow at this temperature.

III. DISCUSSION

The symmetry space group of β-rhombohedral boron is $R\bar{3}m$ (group # 166). To preserve rhombohedral symmetry in the primitive cell, every Wyckoff position must be fully occupied or fully vacant. If the favored structure occupies only a subset of the sites in one or more Wyckoff position, the symmetry is necessarily lower. Our optimal vacancy-ordered structure within the primitive cell yields space group P1 (group #1) corresponding to no point symmetry whatsoever.

According to Landau theory [33] changes of symmetry occur through thermodynamic phase transitions, implying that the β-rhombohedral structure is not the low temperature stable phase. Experimental observation of β as stable indicates either that vacancies are frozen in a disordered arrangement or that β is stabilized by a symmetry-restoring phase transition at some low temperature. This conclusion holds regardless of whether we have found the true optimal structure, since all energetically plausible variants of β lack full symmetry.

The transition temperature is only a crude estimate because of several approximations. We consider only the coupling of primitive cells. We consider only a small fraction of all configurations within these two cells. We neglect atomic vibrations which contribute strongly to the free energy [7, 10] and must be included in any attempt to estimate an accurate transition temperature. However, while the α and β phases differ strongly in vibrational free energy, the ensemble of nearly optimal symmetry-broken β variants most likely remains nearly degenerate in vibrational free energy because their local environments are so similar.

Because our calculated energy differences are at the borderline of reliability of density functional methods it would be desirable to study these energies using more sophisticated quantum chemical methods. Unfortunately at present these methods cannot be reliably applied to periodically repeated crystal structures of the necessary complexity. Although details of the optimal structures may change, our primary conclusions are unlikely to be altered by higher accuracy. The true ground state will be either symmetry-broken β or perhaps α. In either case a phase transition is necessary to recover the experimentally observed equilibrium state above some moderate temperature.

Even within the density functional theory limitations there remains some uncertainty concerning the optimal structure. Within a single primitive cell we have only explored a fraction of all configurations and some other unexamined structure might turn out to be prefered. Among supercells we have only addressed the hexagonal unit cell and the 2x1x1 supercell. It is quite possible that a larger supercell will be even more favorable. In fact it could be that the true ground state even restores rhombohedral symmetry, though in a supercell so that it is no longer the β structure.

In conclusion, we show that suitably resolving correlations among partially occupied sites of β yields an optimal structure whose energy is lower than α. This structure breaks the symmetry of β because it uses only subsets of the fully symmetric Wyckoff positions. Further, we demonstrate the likelihood of superlattice ordering. We propose that the full symmetry of β is restored at moderate temperatures through a phase transition driven by the entropy of partial site occupation.

Acknowledgments

This research was supported in part by the NSF under grant DMR-0111198. We acknowledge useful discussions with B. Widom

---

[1] J. L. Hoard, S. Geller, and R. E. Hughes, J. Am. Chem. Soc. **73**, 1892 (1951).

[2] J. L. Hoard, R. E. Hughes, and D. E. Sands, J. Am. chem. Soc. **80**, 4507 (1958).

[3] L. V. McCarty, J. S. Kasper, F. H. Horn, B. F. Decker, and A. E. Newkirk, J. Am. Chem. Soc. **80**, 2592 (1958).

[4] B. F. Decker and J. S. Kasper, Acta Cryst. **12**, 503 (1959).

[5] R. E. Hughes, C. H. L. Kennard, D. B. Sullenger, H. A. Weakliem, D. E. Sands, and J. L. Hoard, J. Am. Chem. Soc. **85**, 361 (1963).

[6] M. Vlasse, R. Naslain, J. S. Kasper, and K. Ploog, J. Solid State Chem. **28**, 289 (1979).

[7] A. Masago, K. Shirai, and H. Katayama-Yoshida, Phys. Rev. B **73**, 104102 (2006).

[8] M. Mihalkovic and M. Widom, Phys. Rev. B **70**, 144107 (2004).

[9] D. L. V. K. Prasad, M. M. Balakrishnarajan, and E. D. Jemmis, Phys. Rev. B **72**, 195102 (2005).

[10] M. J. van Setten, M. A. Uijttewaal, G. A. de Wijs, and R. A. de Groot, J. Am. Chem. Soc. **129**, 2458 (2007).

[11] H. Werheit and R. Franz, J. Less-Common Met. **117**, 163 (1986).

[12] H. C. Longuet-Higgins and M. de V. Roberts, Proc. Roy. Soc. London A **230**, 110 (1955).

[13] W. N. Lipscomb, J. Less-Common Met. **82**, 1 (1981).

[14] E. D. Jemmis and M. M. Balakrishnarajan, J. Am. chem. Soc. **123**, 4324 (2001).

[15] A "Wyckoff position" is a group of symmetry-equivalent atomic sites.

[16] D. Geist, R. Kloss, and H. Follner, Acta Cryst. **26**, 1800 (1970).

[17] J. L. Hoard, D. B. Sullenger, C. H. L. Kennard, and R. E. Hughes, J. Solid State Chem. **1**, 268 (1970).

[18] B. Callmer, Acta Cryst. B **33**, 1951 (1977).

[19] G. A. Slack, C. I. Hejna, and J. S. Kasper, J. Solid State Chem. **76**, 52 (1988).

[20] G. Kresse and J. Furthmuller, Phys. Rev. B **54**, 11169 (1996).

[21] P. Blochl, Phys. Rev. B **50**, 17953 (1994).

[22] G. Kresse and D. Joubert, Phys. Rev. B **59**, 1758 (1999).

[23] J. P. Perdew and Y. Wang, Phys. Rev. B **45**, 13244 (1992).

[24] I. Boustani, Chem. Phys. Lett. **233**, 273 (1995).

[25] B. Marlid, K. Larsson, and J.-O. Carlsson, Phys. Rev. B **64**, 184107 (2001).

[26] A. Boustani, Phys. Rev. B **55**, 16426 (1997).

[27] D. M. Ceperly and B. J. Alder, Phys. Rev. Lett. **45**, 566 (1980).

[28] D. Vanderbilt, Phys. Rev. B **41**, 7892 (1990).

[29] http://cms.mpi.univie.ac.at/vasp/vasp/node239.html.

[30] M. Mihalkovič and M. Widom, Energetic and structural details are available at web site http://alloy.phys.cmu.edu/published.

[31] S. Chacko, D. G. Kanhere, and I. Boustani, Phys. Rev. B **68**, 035414 (2003).

[32] T. Lundstrom, B. Lonnberg, and J. Bauer, J. All. Comp. **267**, 54 (1998).

[33] L. D. Landau and E. M. Lifshitz, *Statistical Physics* (Pergamon, Oxford, 1969).

Name	Pearson	Atoms	V	$E-E_\alpha$	ΔR	Comments
α-T	tP50	50	7.67	91.91	full occupation	
β-T	tP196	192	7.53	15.13	optimized occupation	
β-R	hR105	105	7.72	25.87	full occupation	
α-R	hR12	12	7.18	0.00	full occupation	
β-R	hR111	105	7.69	13.02	B13bcdefB16a	
β-R	hR111	106	7.64	0.15	B13bcdefB16bd	
β-R	hR141	107	7.57	-0.86	B13bcefB16bdB17aB18a	
β-R	hR141	108	7.56	1.43	B13bcefB16acdB17aB18a	
2x1x1	aP282	214	7.57	-1.75	optimized supercell	

TABLE I: Structural data including atoms per primitive cell, volume (Å^3/atom) and energy relative to α-R (meV/atom). ΔR (Å) measures the deviation of the symmetry-averaged relaxed positions from the crystallographically reported positions, averaged over the fully occupied Wyckoff positions. Comments list occupied sites using notation in Fig. 3. From top to bottom: tetragonal, fully occupied rhombohedral, rhombohedral symmetry-broken structures and our optimized supercell structure.

ΔE	$E_\beta - E_\alpha$				$E_{opt} - E_\alpha$			
E_{cut}	319 eV		415 eV		319 eV		415 eV	
Precision	Med	Acc	Med	Acc	Med	Acc	Med	Acc
k=1x1x1	-7.76	-7.54	-7.98	-7.97	-17.27	-17.08	-17.04	-17.15
k=2x2x2	23.58	23.78	23.85	23.77	-1.71	-1.47	-1.47	-1.68
k=3x3x3	25.71	25.88	26.09	25.99	-1.05	-0.86	-0.65	-0.85
k=4x4x4	25.29	25.39	25.65	25.49	-1.04	-0.88	-0.64	-0.87

TABLE II: Test of convergence as function of energy cutoff, VASP precision setting and k-point mesh. Energies of hR105 (E_β) and our optimal B13bcefB17aB18a structure (E_{opt}) are compared with hR12 (E_α).

ΔE	$E_\beta - E_\alpha$		$E_{opt} - E_\alpha$	
Precision	Medium	Accurate	Medium	Accurate
LDA	47.83	47.86	15.48	15.46
USPP	27.82	27.56	-0.25	-0.45
HARD	36.06	25.94	-0.59	-0.75

TABLE III: Test of alternate potentials. All calculations are done with a 3x3x3 mesh at the default energy cutoff. USPP and HARD use the PW91 GGA. LDA and HARD use PAW potentials.

B13 sites	B16 sites	Atoms	$E - E_\alpha$
a b c d e f		105	25.84
a b c d e f	a	106	12.25
a b c d e f	b d	107	12.50
b c d e f		104	27.38
b c d e f	a	105	13.02
b c d e f	a b	106	13.81
b c d e f	b	106	13.10
b c d e f	b d	106	0.15
b c d e f	b e	106	5.21
b c d e f	b f	106	0.87

TABLE IV: Table of selected data for hR111. (top) Full B13 occupation; (middle) Single B13 vacancy with single or double occcupation of one B16 triangle; (bottom) Single occupancy of both B16 triangles. Energy units are meV/atom.

B13 sites	B16 sites	B17	B18	B19	B20	Atoms	$E - E_\alpha$
a b c d e f	b d	a				108	6.62
b c d e f	b d	a				107	20.29
b c e f	b d	a				106	0.15
b c e f	a d	a	a			107	-0.07
b c e f	b d	a	a			107	-0.86
b c e f	c d	a	a			107	3.48
b c e f	b d			a		106	12.96
b c e f	b d	a	a		h	108	0.844

TABLE V: Table of selected data for hR141. (top) B13 vacancies; (middle) B16 occupation; (bottom) Structures occupying B19 and B20 sites. Energy units are meV/atom.

B13(1)(2)(3)	B16(1)(2)(3)	B17B18(1)(2)(3)	Atoms	ΔE
(bcef)(bcef)(bcef)	(bd)(bd)(bd)	(aa)(aa)(aa)	321	0
(bcef)(acde)(bcef)	(bd)(cf)(bd)	(aa)(bb)(aa)	321	0.09
(bcef)(acde)(abdf)	(bd)(cf)(ae)	(aa)(bb)(cc)	321	0.31

TABLE VI: Hexagonal unit cell energies. Site occupancy is given for each primitive cell, (1), (2) and (3). ΔE is relative to a supercell of the optimal 107 atom hR141 structure, in units of meV/atom.

B13(1)(2)	B16(1)(2)	B17B18(1)(2)	Ω	ΔE
(bcef)(acde)	(ad)(bd)	(aa)(bb)	8	-0.89
(bcef)(acef)	(ad)(bd)	(aa)(bb)	4	-0.75
(bcef)(bcdf)	(ce)(ad)	(aa)(ee)	8	-0.24
(acde)(bcdf)	(bd)(ad)	(bb)(ee)	8	-0.11
(bcef)(bcef)	(bd)(bd)	(aa)(aa)	12	0.00

TABLE VII: Selected 2x1x1 supercell energies, including multiplicities Ω. ΔE is relative to a doubling of the optimal 107 atom hR141 structure, in units of meV/atom.

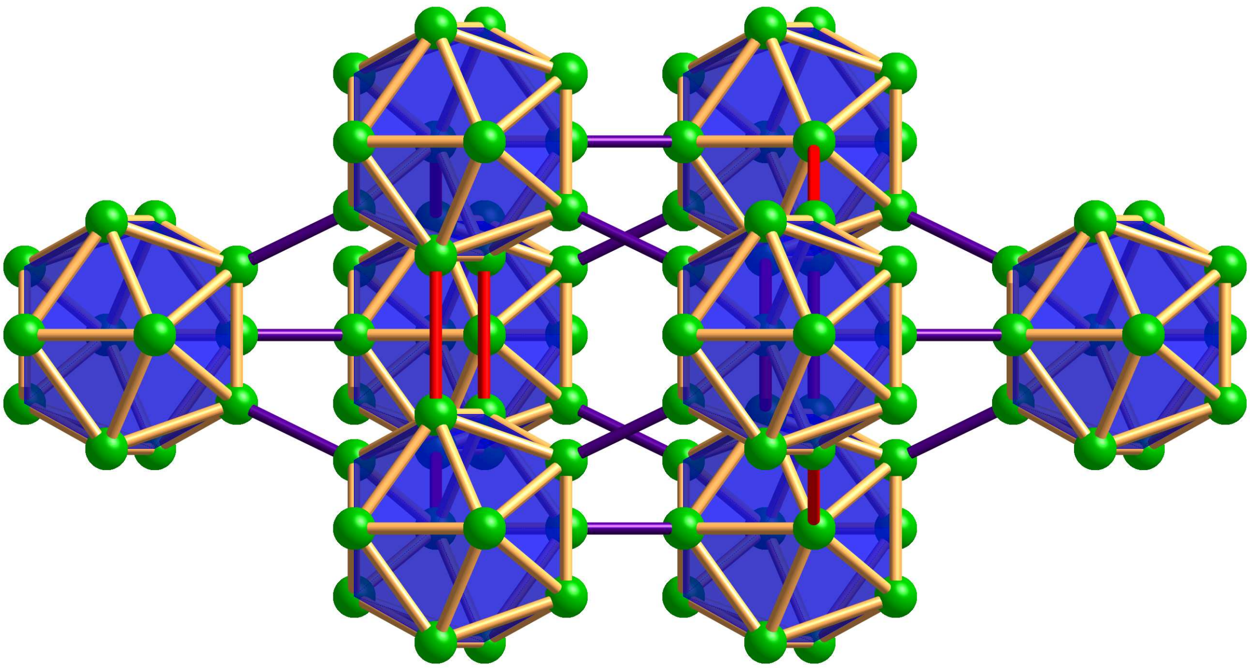

FIG. 1: Structure of α-rhombohedral boron viewed along the rhombohedral $(11\bar{2})$ axis. Bond color scheme: 1.67 Å in purple; 1.75-1.81 Å in orange; 2.01 Å in red.

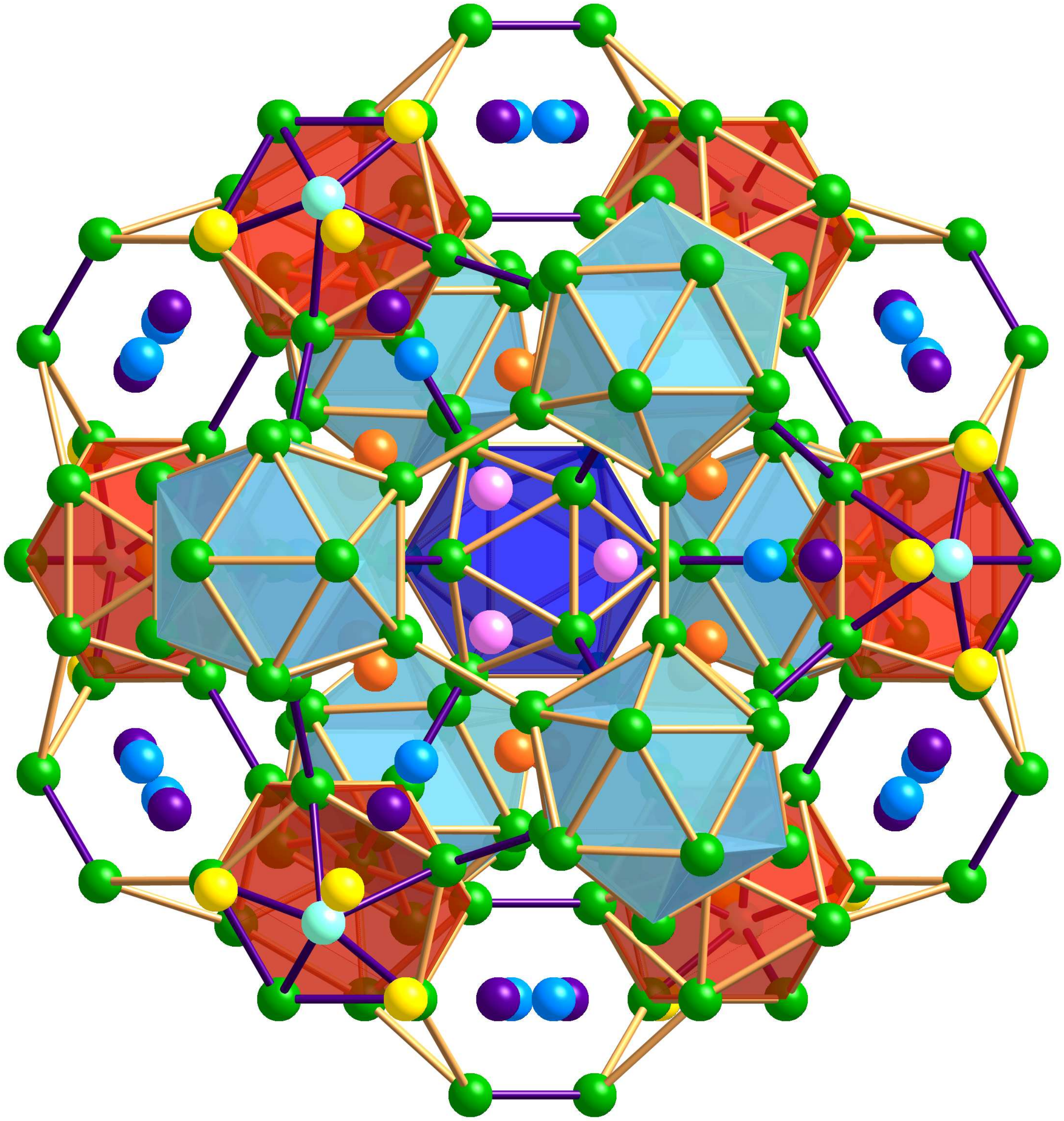

FIG. 2: Structure of β-rhombohedral boron viewed along rhombohedral (111) axis. Bond color scheme: 1.63-1.73 Å in purple; 1.73-1.92 Å in orange. Partially occupied sites (see text) are shown in color: B13 (74.5% average occupancy) cyan; B16 (27.2%) pink; B17 (8.5%) yellow; B18 (6.6%) indigo; B19 (6.8%) blue; B20 (3.7%) orange.

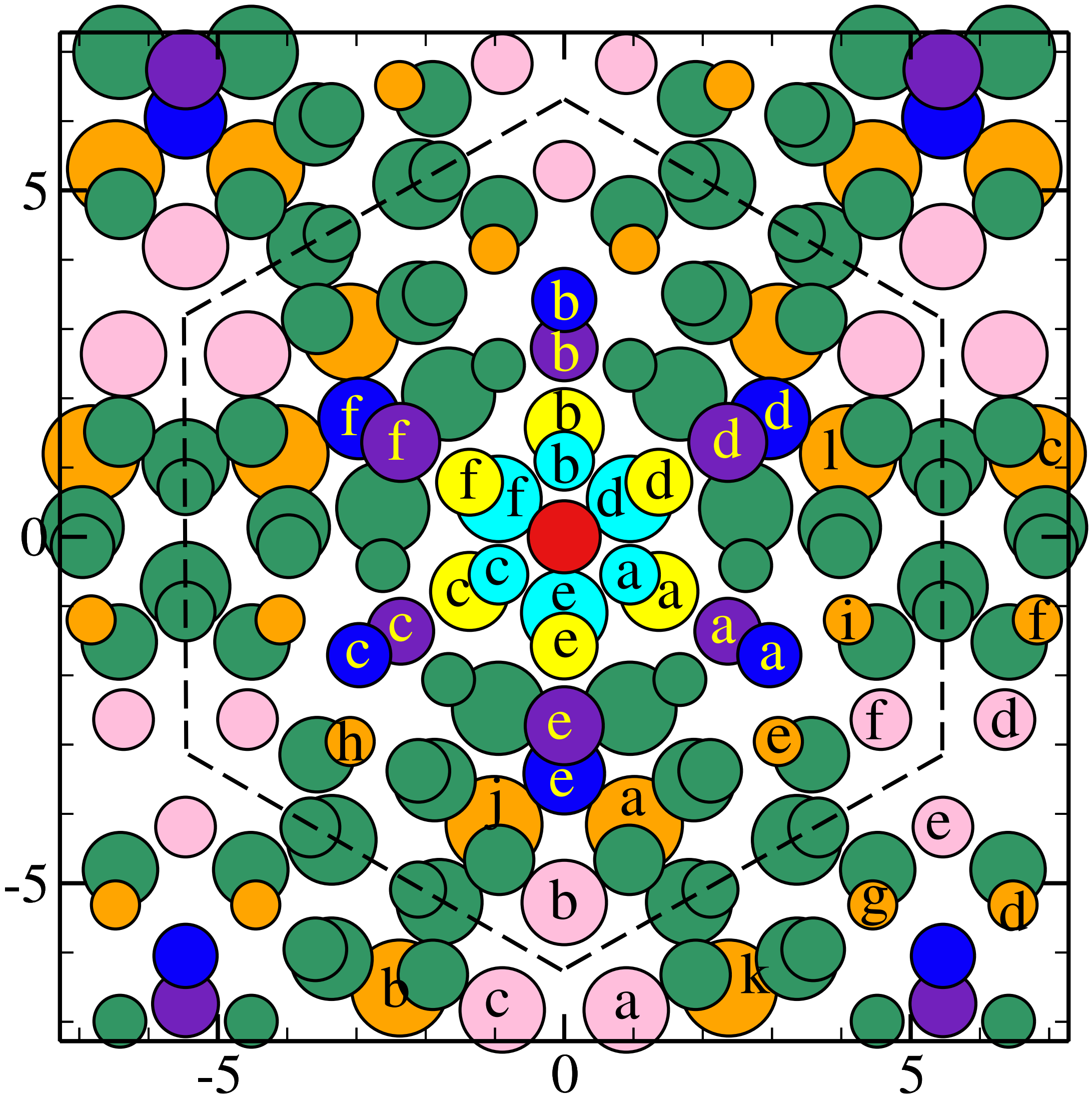

FIG. 3: Structure of β-rhombohedral boron in vicinity of cell body center (B15, shown in red) viewed along the rhombohedral (111) axis. Color coding as in Fig. 2. Site labels correspond to notation in table I. Size of atoms indicates vertical position, with small on top. Length scale is in Angstroms. The dashed lines contains a single hexagonal unit cell.

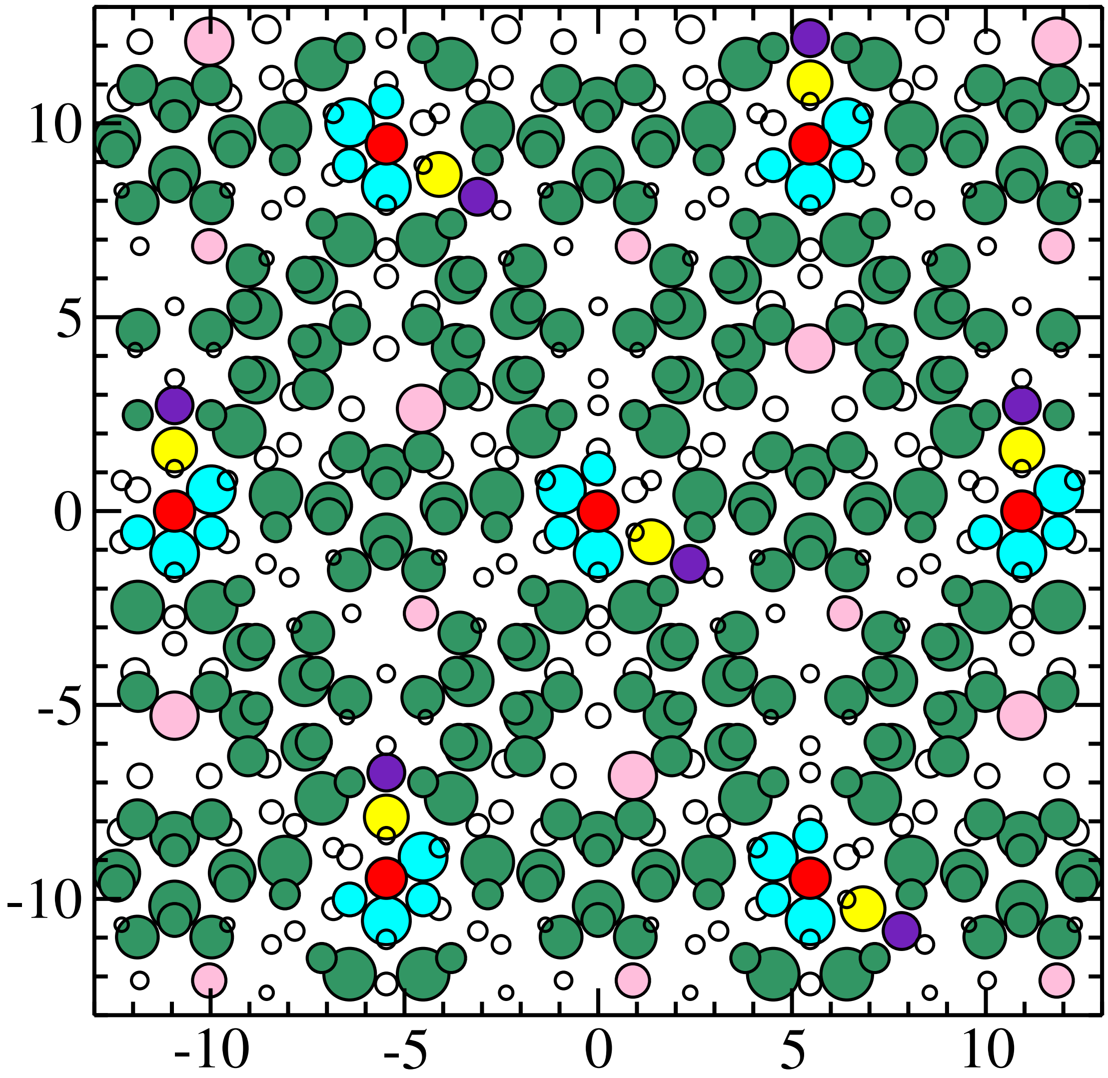

FIG. 4: Optimal site occupation of a β-rhombohedral 2x1x1 supercell viewed along the rhombohedral (111) axis. Color coding as in Fig. 3. Small empty circles locate vacant sites.

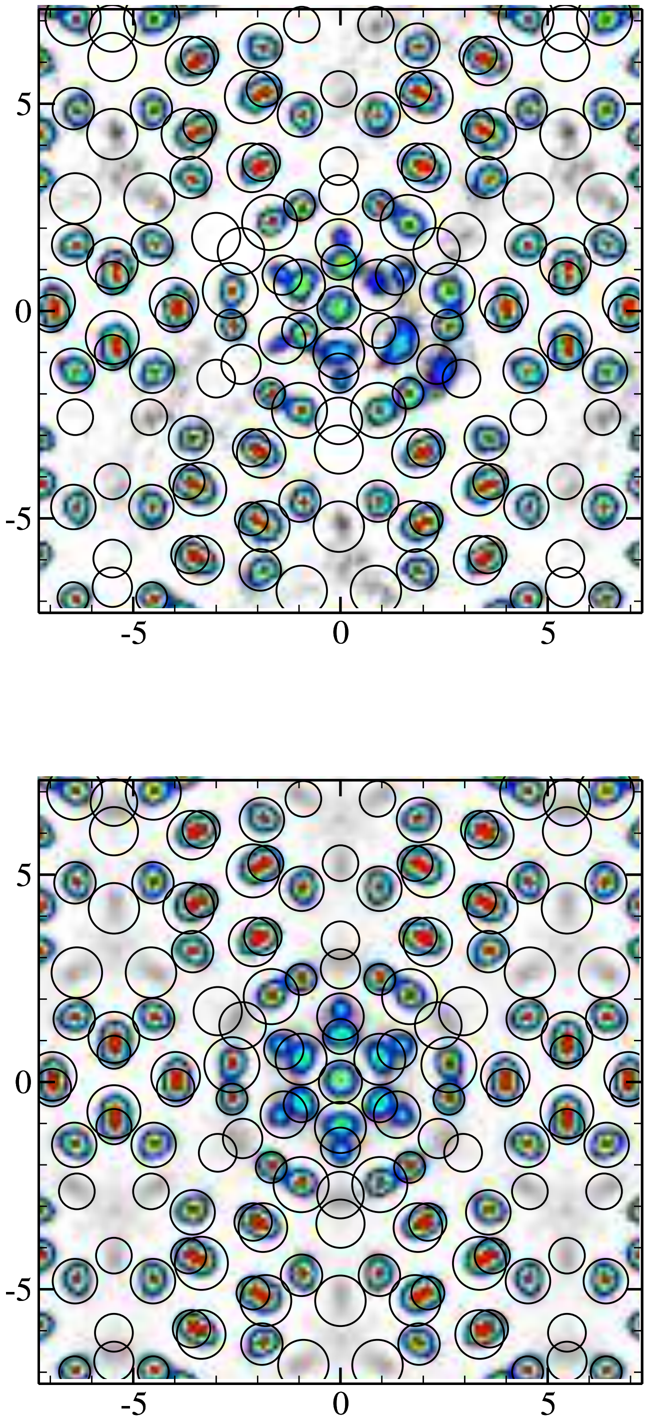

FIG. 5: Density plot of simulated atomic positions. Grayscale indicates low frequency positions, colors indicate medium (blue) - high (red) frequency positions. Crystallographically determined atomic positions are superimposed (and suitably scaled) for comparison with Fig. 3. (top) Run started in optimal configuration. (bottom) Same data with rhombohedral symmetry imposed by averaging.

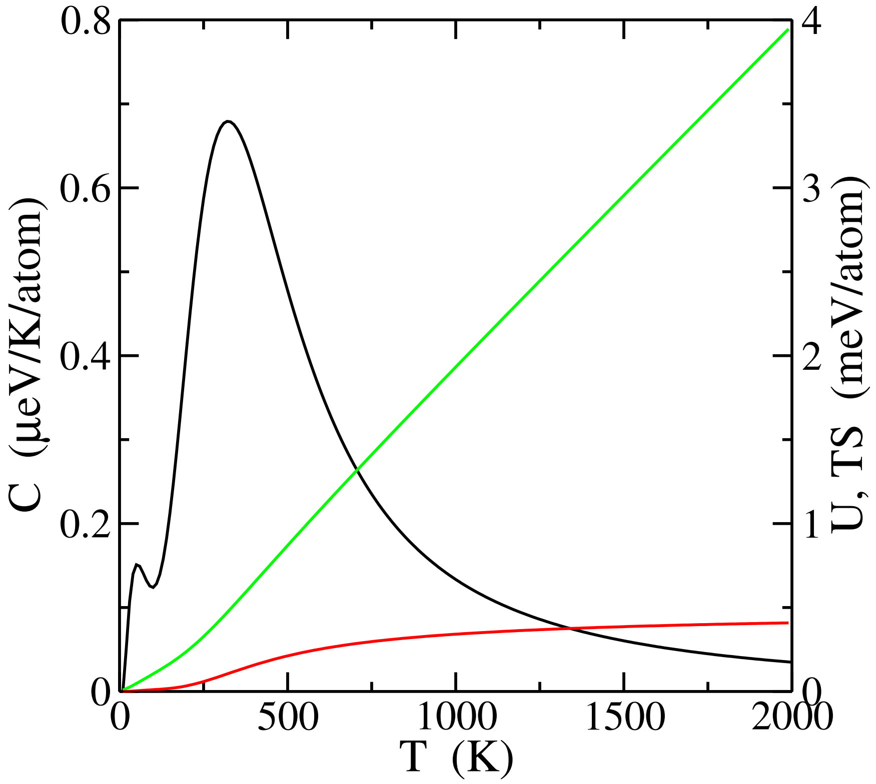

FIG. 6: Heat capacity (black), energy (red) and entropy (green) of supercell model. Energy is relative to the optimal supercell structure.